Available online at www.sciencedirect.com
SCIENCE DIRECT®
Vision Research 45 (2005) 617–633
Vision Research
www.elsevier.com/locate/visres

"Crowding" in normal and amblyopic vision assessed with Gaussian and Gabor C's

Srividhya Hariharan [a], Dennis M. Levi [b,*], Stanley A. Klein [b]

[a] College of Optometry, University of Houston, Houston, TX 77204-6052, USA
[b] School of Optometry and Helen Wills Neuroscience Institute, University of California, Berkeley, CA 94720-2020, USA

Received 17 March 2004; received in revised form 11 September 2004

Abstract

The purpose of this study was to investigate the extent and specificity of crowding in the normal fovea and periphery, and the central field of amblyopes, using "C"-like patterns. In the first experiment we measured the extent of crowding for C-patterns comprised of Gaussian patches, over a range of target sizes using a four-alternative forced-choice (up, down, left, right) method. We found that the extent of foveal crowding is proportional to target size. In contrast, in normal periphery and in the central field of amblyopes, crowding extends over large spatial distances and is not size dependent. Crowding for our stimuli occurred with both same-polarity and opposite polarity patches. To test whether the extended crowding in amblyopia resulted from a shift in the spatial scale of analysis, we measured crowding with band-limited C-patterns (comprised of Gabor patches) in a gap localization task (2-AFC). With band-limited stimuli, and a task that does not involve judging the orientation of the gap, the amblyopic eyes showed crowding over a longer distance than that of normal observers. We also tested the orientation specificity of crowding by varying the orientation of the flanks. In normal fovea, crowding is orientation specific: in amblyopia it is not. While crowding in normal fovea can be explained by simple pattern masking, crowding seen in normal periphery and amblyopes cannot. Instead we suggest that crowding in amblyopic and peripheral vision is a result of extended pooling at a stage following the stage of feature detection.

Keywords: Amblyopia; Peripheral vision; Crowding; Contour interaction; Masking; Psychophysics

1. General introduction

The deleterious influence of nearby flanks on visual discrimination is known as contour interaction or "crowding". In peripheral (Bouma, 1970; Levi, Klein, & Aitsebaomo, 1985) and amblyopic vision (Flom, Weymouth, & Kahneman, 1963; Hess & Jacobs, 1979; Levi & Klein, 1985) crowding can occur over long distances. Crowding has been extensively studied, but is not fully understood. In a recent study, we used E-like targets comprised of Gaussian or Gabor patches, and showed that in foveal vision, the extent of crowding is proportional to target size over a 50-fold range of target sizes, and that it is readily explained by simple contrast masking (Levi, Klein, & Hariharan, 2002). In contrast, in peripheral and amblyopic vision (Levi, Hariharan & Klein, 2002a, 2002b) we found that crowding extended over a larger spatial distance, and could not be simply explained on the basis of simple contrast masking.

In the present paper we report the results of crowding experiments conducted on normal fovea, periphery and central field of strabismic amblyopes using a "C-pattern". We chose the "C-pattern" for several reasons: (1) it is localized and highly familiar, (2) a number of studies including the classical study by Flom et al. (1963) as well as recent studies by Hess and colleagues

* Corresponding author. Tel.: +1 510 6423414; fax: +1 510 6427806.
E-mail address: dlevi@berkeley.edu (D.M. Levi).

0042-6989/$ - see front matter © 2004 Elsevier Ltd. All rights reserved.
doi:10.1016/j.visres.2004.09.035

(Hess, Dakin, & Kapoor, 2000; Hess, Dakin, Kapoor, & Tewfik, 2000; Hess, Dakin, Tewfik, & Brown, 2001; Hess, Williams, & Chaudhry, 2001) have used Landolt C targets to study the effects of nearby contours on visual discrimination, (3) the C-pattern varies smoothly in space, and is more compact than the "E-pattern" used in our earlier studies (Levi, Klein, & Hariharan, 2002; Levi, Hariharan, & Klein, 2002a, 2002b) because the constituent patches in our sampled C-pattern are overlapped, (4) the C-pattern has a single gap and therefore does not provide the strong global orientation cue that is seen in the E-pattern, (5) our Gaussian C has a significant advantage over the sharp-edged letters that are typically used, since it is low-pass, thus reducing the importance of high spatial frequencies. As clearly shown by Hess et al. (2001), with sharp-edged C's, there is a strong effect of spatial frequency as the target size is varied whereby for tiny letters optical blur strongly attenuates high frequency features.

2. General methods

The stimuli, comprised of Gaussian (Fig. 1) or Gabor (Fig. 2) patches, were displayed on a video monitor (either a Monoray high brightness monitor with a mean luminance of approximately 80 cd/m^2 or a Mitsubishi Diamond Scan 20H monitor with a mean luminance of approximately 56 cd/m^2) using a Cambridge Research Systems VSG 2/3 graphics card with 15-bit contrast resolution. Six control observers (including two of the authors) with normal or corrected-to-normal vision participated in one or more of the experiments and three amblyopic observers with varying degrees and types of amblyopia participated in these experiments. A detailed description of the type and degree of amblyopia and other specifics for the amblyopic observers can be found in Table 1. For peripheral viewing, the stimuli were presented at 5 deg in the lower visual field. For all observers, viewing was monocular, with the untested eye occluded with a black patch. All observers were well trained in making psychophysical judgements.

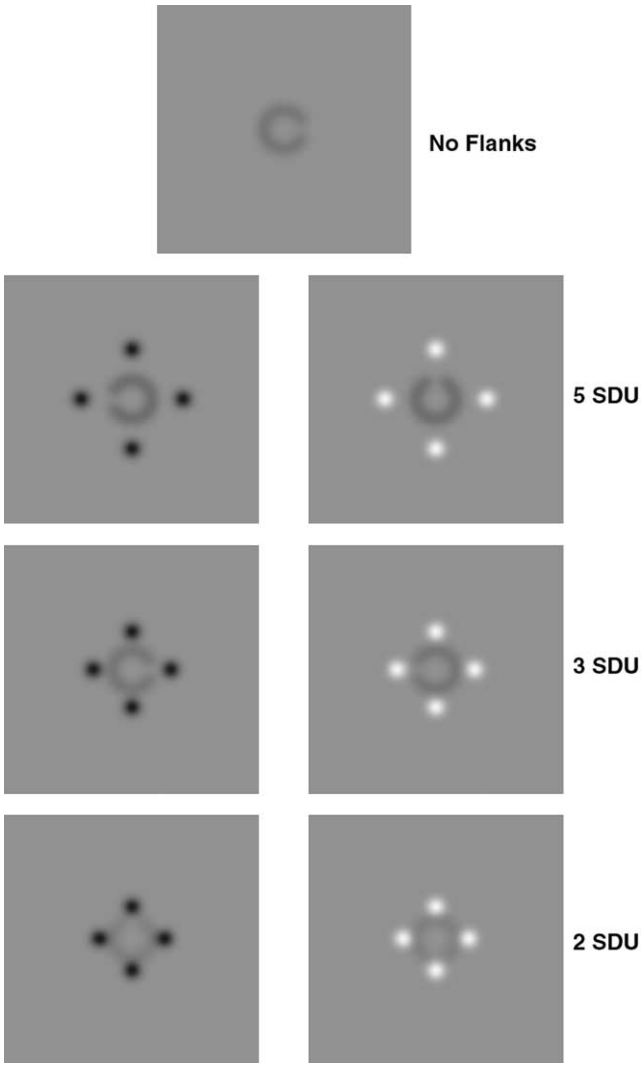

Fig. 1. Examples of Gaussian "C" stimuli used in Experiment 1. The top panel is the isolated C made of twelve equally spaced (30 deg of angular separation) circular dark Gaussian patches with one missing patch, which served as the target. The other panels show C's surrounded by high contrast flanks at separations equal to 5, 3 and 2 standard deviation units (target to flank distance/ standard deviation of the patch) from the target. The left panels show C targets surrounded by same polarity flanks; the right panels, opposite polarity flanks.

3. Experiment 1—Crowding with Gaussian "C-patterns" of different sizes

Flom et al. (1963) reported that the extent of crowding was proportional to the minimum angle of resolution (MAR) in normal and amblyopic observers using Landolt C targets. Based on these findings they concluded that the extent over which crowding occurs might be related to the size of the receptive field (and hence the resolving capacity) associated with the retinal region used to fixate the target. In normal periphery and central field of amblyopes, small receptive fields have low sensitivity. Therefore, larger receptive fields are engaged, resulting in reduced visual acuity or increased MAR. This putative shift from small to large receptive fields is commonly known as the "scale shift" hypothesis (Levi & Waugh, 1994; Levi, Waugh, & Beard, 1994). However, Flom et al., and until very recently (see below) almost all other studies of crowding used targets that were at or near the observer's acuity limit. Since acuity is reduced in peripheral and amblyopic vision, the increased extent of crowding might simply be a consequence of using larger targets to test amblyopic and peripheral vision because of their reduced acuity. One needs to vary stimulus size as an independent variable.

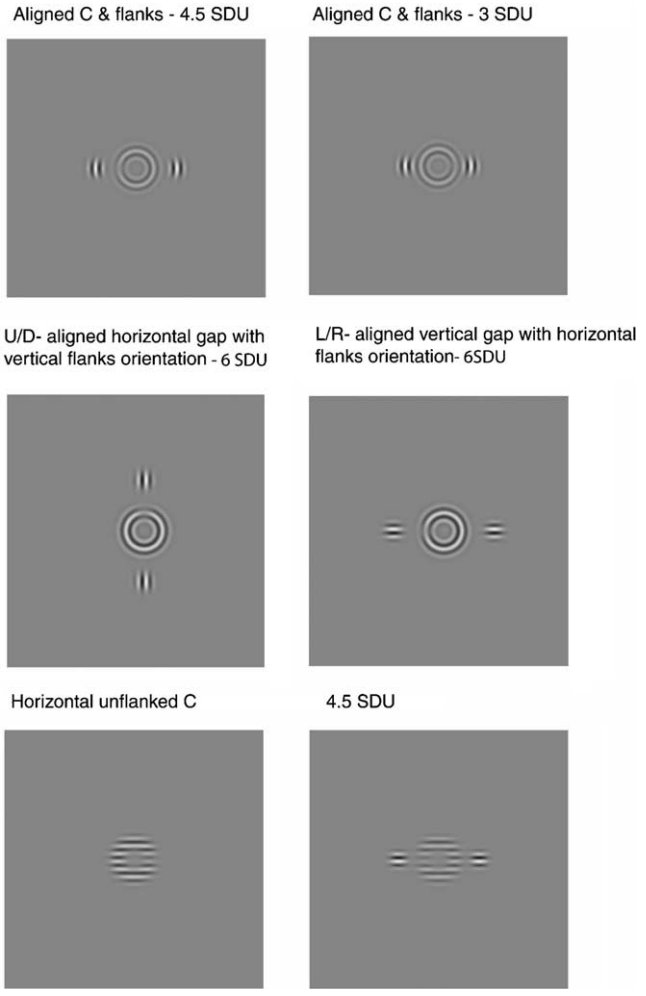

Fig. 2. Examples of band-limited C targets made of twelve equally spaced (30 deg of angular separation) Gabor patches with one missing patch with varying orientations used in Experiment 2. The top panels show C's and flanks at target to flank distances of 4.5 and 3 standard deviation units. The gap orientation of the C and flanks are similar in the top panels. The middle panels show C's at target to flank distances of 6 standard deviation units and the gap orientation of the C is orthogonal to the orientation of the flank. The bottom panels show examples of unflanked C targets (left) and C target with flanks at 4.5 standard deviation units made of horizontally oriented Gabor patches, which was used to measure extent of crowding in the 180 deg direction-identification task.

Based on the scale shift hypothesis and Flom et al.'s suggestion (the extent of interaction being proportional to the size of the receptive field) we can make two predictions on the nature of crowding in amblyopes and periphery of the normal observers. The first prediction is that the spatial extent of crowding will depend on the size or the spatial frequency of the target. Several very recent studies have looked at how crowding depends on target size. Levi, Klein, and Hariharan (2002) showed that in normal foveal vision, crowding depends on target size over a 50-fold range of target sizes. However, in peripheral and amblyopic vision (Levi, Hariharan, & Klein, 2002a, 2002b) crowding extended over a large fixed distance, and showed little or no dependence on target size. Levi et al. used E patterns, and, as noted above, the results may not generalize to other targets. Similarly, Tripathy and Cavanagh (2002) found that the extent of crowding for T' targets, by 'squared-thetas' as flanks in peripheral vision, did not scale with target size. Tripathy and Cavanagh did not test foveal or amblyopic vision. A second, prediction of the scale-shift hypothesis is that the extent of crowding may be similar in normal and amblyopic vision when targets are large relative to their acuity limit. This prediction is based on the assumption that small receptive fields that can resolve high spatial frequencies are compromised in amblyopic vision, while large receptive fields are intact.

In order to test these predictions we measured crowding with Gaussian "C"-patterns of different sizes. The "target" was a C-like figure comprised of 12 equally spaced (30 deg of angular separation) circular dark Gaussian patches with one missing patch (Fig. 1). The radius of the C was always set to be 3.33 times the patch standard deviation. On each trial the target was presented briefly (for 195 ms) with one of four orientations (up, down, left, right) selected at random. The observer's task was to identify the orientation of the C.

In order to assess the influence of the flanks on pattern perception we measured the contrast thresholds for identifying the orientation of the target by using a

Table 1
Visual characteristics of amblyopic observers

Observer	Age/sex	Eye	Rx.	Acuity[a]	Fixation[b]	Strabismus
Strabismic						
RH	32/M	O.D.	$-1.00/-0.50\times170$	20/15	Central	
		O.S.	$-1.50/-1.50\times10$	20/59	Unsteady	Microtropia l.et., 2Δ
Strab and Aniso						
DS	26/M	O.D.	+2.25 DS	20/40	2 deg Nasal	Constant r.et., 8Δ
		O.S.	+0.50 DS	20/20	Central	
DM	40/F	O.D.	$-0.50/-0.25\times92$	20/20	Central	
		O.S.	$-2.50/-1.00\times160$	20/80	0.5 deg Nasal	Constant l.xt., 3Δ

[a] 75% correct on Davidson–Eskridge charts.
[b] Fixation determined with Haidinger's brushes and Visuoscopy.

four-alternative forced choice method of constant stimuli. The four surrounding flanks were comprised of one Gaussian patch each (Fig. 1). The standard deviation of the flanker was the same as that of the constituent Gaussians comprising the C. Unless otherwise specified, the polarity of the flanks were identical to that of the target (which was always dark), and the flank contrast was 90%. From trial to trial, the target was presented at one of four near-threshold contrast levels (based on pilot experiments), and the resulting psychometric function was fit with a Weibull function in order to estimate the threshold for identifying the orientation of the target. Each threshold estimate, corresponding to the contrast resulting in 72.4% correct performance ($d' = 1.6$), was based on 100 trials. The contrast thresholds presented in the results section are the weighted means of at least four individual threshold estimates. From one run to another, we varied the flank distance (including infinity which provided a measure of unflanked performance) and the viewing distance in order to vary the target size. The flank distance was specified as the distance from the center of the flank to center of the adjacent C patch (or gap). Fig. 1 shows examples of an unflanked C, which was used as the target and a C with flanks at distances corresponding to 5, 3 and 2 times the patch standard deviation units (SDU, i.e., target to flank distance divided by standard deviation of the patch). In the opposite-polarity experiment, the flanks were bright, while the C was still dark (shown in the right panels of Fig. 1). Three normal and three amblyopic observers were tested with two different target sizes. We also obtained fragmentary data on a fourth normal observer.

We also measured the minimum angle of resolution (MAR) for unflanked Gaussian C-like targets at 70% contrast. The percentage of correct responses for identifying the orientation of the C's of different sizes in 0.1 log unit steps was measured. The MAR was estimated by fitting the data with a Probit function. The threshold estimates were based on 200–400 trials for each target size, and is specified as 1/12 of the circumference of the just discriminable C. We measured MAR using Gaussian C's for one control (SH) and all the amblyopic observers.

4. Results and discussion—Experiment 1

We define crowding as the increase in the contrast thresholds for identifying the orientation of the C-pattern in the presence of nearby flanks. In normal foveal vision, both the unflanked threshold and the flank-to-target distance at which thresholds begin to rise depends on the target size. This can be seen in Fig. 3 which shows foveal performance (open symbols) for Gaussian C's for a range of target sizes. Note that for the normal fovea, in the crowded region thresholds are more or less independent of target standard deviation, and the slopes of the threshold vs. separation curves are ≈ -1. In this regime, the product of flank distance and contrast threshold is approximately constant. We suspect that this reflects an "intrinsic blur" for crowding. In contrast, in peripheral vision, for a given target size (Fig. 3 filled symbols), crowding extends over considerably larger distances than in the fovea (open symbols). In striking similarity, for a given target size, the amblyopic eye (Fig. 4 solid symbols) shows a greater extent of crowding when compared to the non-amblyopic eye, as seen by the upward and rightward shift of the data. In order to assess the predictions of the scale-shift hypothesis, we quantified the extent of crowding by fitting Gaussian functions to the data (Eq. (1), shown by the lines in Figs. 3 and 4). We specify the critical distance (CD) as the flank distance that causes the unflanked thresholds to double.

$$\mathrm{Th_f} = \mathrm{Th_{unf}} * (1 + \mathrm{Peak}^{\wedge}(1 - (\mathrm{FD}/\mathrm{CD})^2)) \quad (1)$$

where $\mathrm{Th_f}$ is the flanked threshold, $\mathrm{Th_{unf}}$ is the unflanked threshold, Peak is the peak amplitude of the Gaussian, and FD is the flank distance. It is important to note that the fit was not constrained to pass through the measured unflanked threshold (triangles in Figs. 3 and 4). The critical distance (in minutes) is plotted as a function of target size (minutes) in Fig. 5. The present study shows that in normal foveal vision (Fig. 5, thin symbols), the extent of crowding for C-patterns, quantified in terms of the critical distance, is proportional to the target size over the 4-fold range of target sizes that we measured. On the other hand normal periphery (Fig. 5, thick symbols) and amblyopic eyes (Fig. 5, solid symbols) do not show this size dependence. For small targets, crowding in peripheral and amblyopic vision does not scale to target size, but is disproportionately large. Interestingly, for large targets the critical distances for peripheral and amblyopic vision approach those of the normal fovea, consistent with the second prediction of the scale shift hypothesis (i.e., that the extent of crowding may be similar in normal and amblyopic vision when the targets are large).

Flom et al. (1963) showed the extent of interaction to be proportional to the minimum angle of resolution (MAR). Flom et al. estimated (by eye) the extent of interaction based on percentage of correct responses for C's at the observer's acuity limit. They identified the maximum bar separation affording interaction and specified it as point x (percentage of correct responses begin to decline) and the bar separation producing the greatest interaction was designated as point y (percentage of correct responses decreases to or below chance level). Following this they showed that the maximum amount of interaction (point y) was about two times the MAR, while the minimum amount of interaction (point x) was five times the MAR. In order to examine

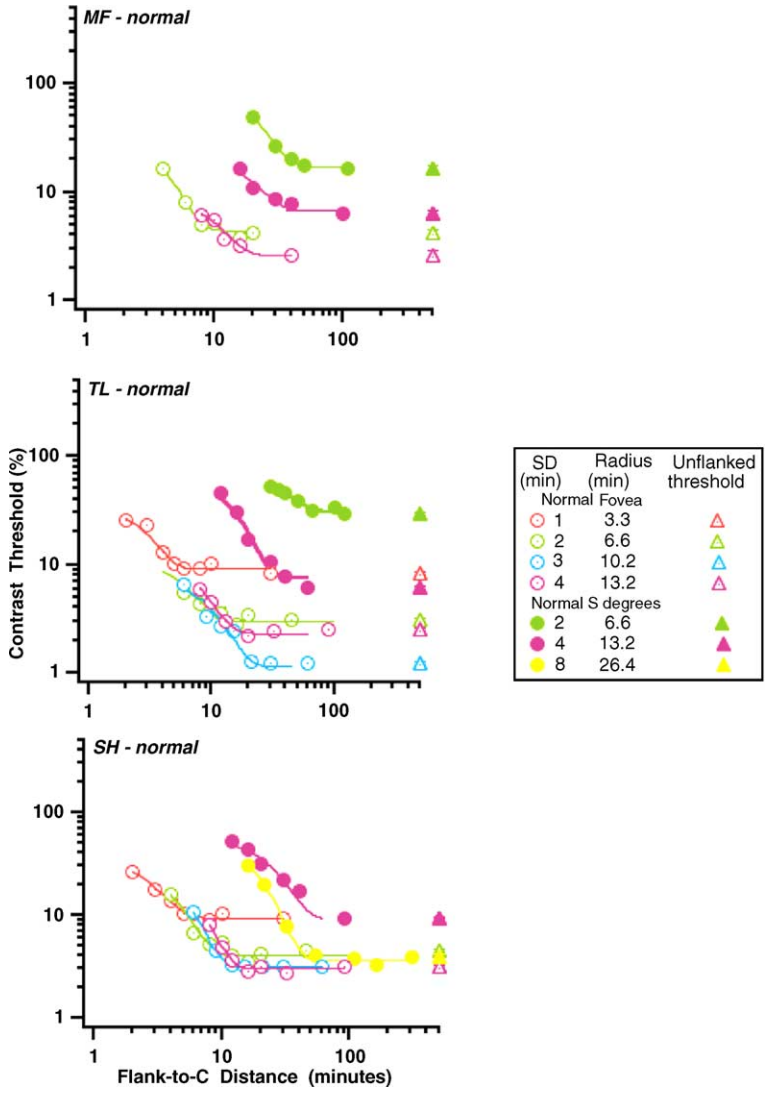

Fig. 3. Contrast thresholds in percentage vs. flank to C distance in minutes of arc for Gaussian C's. Each panel shows data from fovea and periphery (5 deg) for different target sizes (coded by color) in three control observers. In each panel, open symbols represent data from the fovea; solid symbols represent data from the periphery. The triangles (solid-periphery, open-fovea) represent unflanked thresholds (identification thresholds in the absence of flanks) for each target size.

the relationship between the spatial extent of crowding and our observers' MAR, we plot each observer's smallest critical distance against their MAR (Fig. 6). For the two normal observers, the critical distance is approximately 3′, roughly 5–6 times the observers' MAR. For the three amblyopic eyes the MAR is higher, as expected, but the CD is between 7 and 17 times the MAR. We note that two of the non-amblyopic eyes (DS and RH), also shows disproportionately large crowding. Note that Table 1 shows that RH has a four-fold difference of acuity in the two eyes, but Fig. 6 indicates that the MAR's are about the same. This difference reflects the effects of crowding. MAR in Fig. 6 is for isolated C's (see methods), whereas in Table 1 it reflects the acuity on a very crowded Davidson–Eskridge chart.

The two lines in Fig. 6 correspond to the two ratios (points x and y). Considering point x, the maximum bar separation at which interaction occurs, as the extent of interaction, Flom et al. showed that in amblyopic and normal observers point x was 6.8 and 4.7 times the multiple of gap width respectively. Even though the extent of the zone of interaction was larger in angular terms for most amblyopic eyes, it was similar to normals when expressed in multiples of the interaction-free minimum angle of resolution. On the other hand we estimated our extent of crowding based on the point at which the unflanked thresholds doubled (as mentioned earlier). In normal vision, we found that critical distance is proportional to target size so there is no simple relationship between CD and MAR. For example, the measured minimum angle of resolution using the Gaussian C's

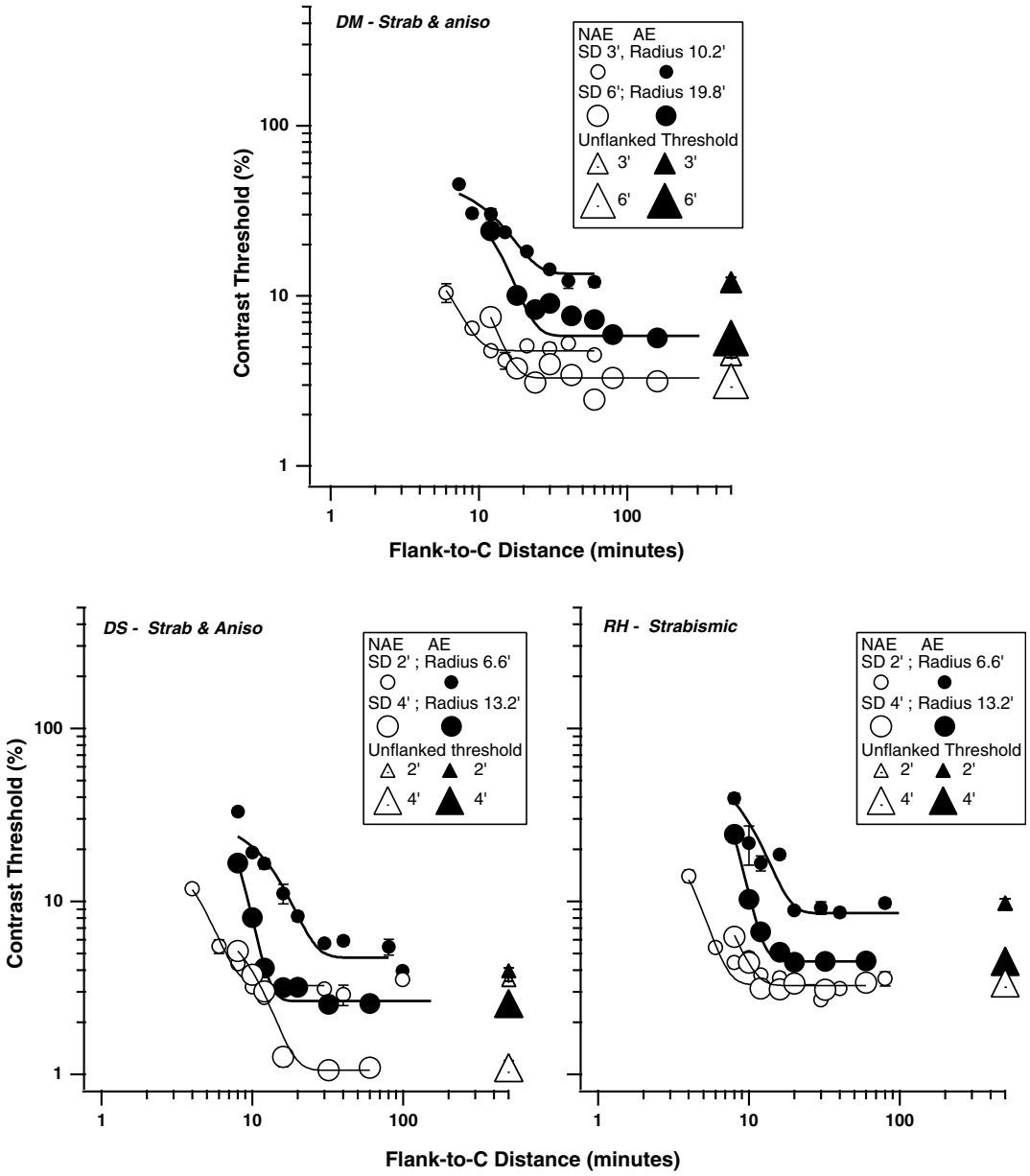

Fig. 4. Contrast thresholds in percentage vs. flank to C distance in minutes of arc tested with Gaussian C's in amblyopic observers. Each panel shows data for both amblyopic and non-amblyopic eyes for different target sizes (coded by symbol size) in three amblyopic observers. In each panel, open symbols represent data from the non-amblyopic eye; solid symbols represent amblyopic eye. The triangles (solid-AE, open-NAE) show unflanked thresholds. Observers RH and DS were tested with same target sizes.

for the control observer SH was 0.6 min. The extent of crowding for this observer was measured and estimated with four different target sizes (C's made of 1′, 2′, 3′ and 4′ standard deviation patches). The smallest size C used to measure the extent of crowding was a C made of twelve 1′ standard deviation patches with one missing patch and according to our estimates the "effective" gap width of this C subtends approximately an angle of 1.7′ (i.e., 1/12 of the circumference of the C) at the fovea. Thus, the gap width of the smallest size C used was almost 3 times the MAR (0.6′ for SH) and the critical distance for the smallest C was about 3′ (or 5 times MAR). The key point is that some amblyopic eyes show a greater extent of crowding than expected based on their MAR. While DM's crowding distance is not much different from the normal observers (after scaling for MAR), both RH and DS have critical distances which are larger. It is also interesting to note that the fellow non-amblyopic eye of observer DS shows an increase in the extent of crowding. Our results, in contradistinction to Flom et al.'s findings show that for small, but suprathreshold targets, amblyopes have a greater extent of crowding than our normal observers when expressed in terms of their minimum angle of resolution. It is also important

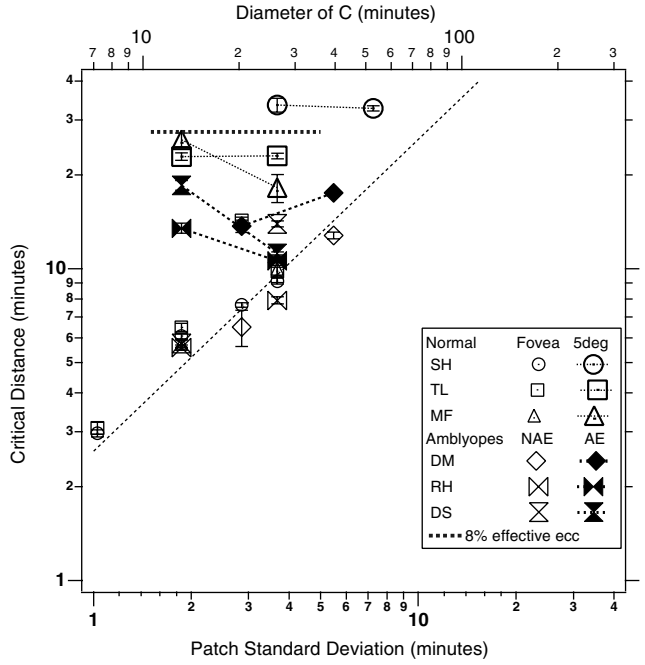

Fig. 5. Critical distance in minutes, representing the extent of interaction for Gaussian C's, is plotted against target size—patch standard deviation (bottom abscissa) or diameter of the C (top abscissa). Thin symbols represent data from normal fovea, thick symbols from normal periphery and solid symbols from amblyopic eyes. Foveal crowding is size invariant but crowding is not size invariant in normal periphery and amblyopic vision. The dotted horizontal line represents the critical distance at 8% of effective eccentricity.

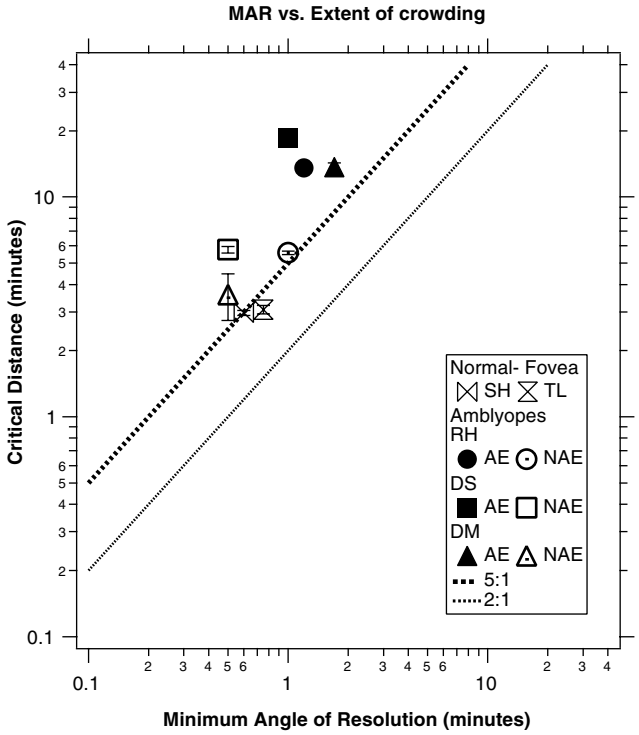

Fig. 6. The critical distance (i.e., the flank distance at which thresholds are elevated by a factor of 2, specified in arc minutes) vs. minimum angle of resolution (minutes) for Gaussian C's for fovea of the control observers (bowtie and propeller), non-amblyopic eyes (open circle, square and triangle) and amblyopic eyes (solid symbols). The thick dotted line is the 5:1 proportionality line, which represents the maximum amount of interaction and the thin dotted line is the 2:1 proportionality line, which represents the minimum amount of interaction (from Flom et al., 1963).

to note that previous studies (Hess & Jacobs, 1979; Latham & Whitaker, 1996; Leat, Li, & Epp, 1999; Hess et al., 2001) have shown crowding to be abnormal in both form and magnitude in some amblyopes and in the periphery of normal observers respectively. Most importantly, in relation to our results they have shown that this abnormality does not depend simply upon the acuity deficit seen in amblyopic and normal peripheral vision.

While the present results are similar to those obtained with E-like patterns (Levi, Klein, & Hariharan, 2002), the effect of the flanks on discriminating the orientation of the C-pattern is different from its effect on the E-pattern. With E-patterns, crowding produces 180 deg (mirror image) errors. In contrast, crowding a C results in, on average, a factor of two more 90 deg than 180 deg errors (as expected based on random performance, since there are twice the number of possible 90 deg confusions). For normals the ratio of 90–180 deg errors was 2.08 ± 0.11; for the preferred eyes of amblyopes, 2.12 ± 0.13, and for the amblyopic eyes, it was 2.06 ± 0.06.

4.0.1. The effect of flank polarity

Flank polarity can have a strong influence on "crowding" (Kooi, Toet, Tripathy, & Levi, 1994). For example, in the normal fovea, reversing the contrast polarity between the targets and the flanks abolished contour interaction for near acuity threshold, sharp-edged Landolt C's (Hess et al., 2000—but see Liu, 2001) but not for suprathreshold C's (Hess et al., 2001). These effects are important, because they suggest that different mechanisms may be at work for near threshold vs. suprathreshold targets. Moreover, opposite-polarity flanks had different effects in amblyopic and peripheral vision (Hess, Dakin, & Kapoor et al., 2000; Hess et al., 2001). We wondered whether the differential effects of polarity in normal and amblyopic crowding might be due to the sharp-edged targets used by Hess and colleagues. Therefore we tested the effect of flank polarity in our normal observers by measuring crowding with Gaussian C's and opposite polarity Gaussian flanks. Fig. 7 shows mean threshold elevation from the fovea of three normal observers and data from 1 amblyope DS for same and opposite polarity conditions. Threshold elevation was generally similar with the same- (dark C and dark flanks) and opposite-polarity (dark C and bright flanks) for the nearthreshold C (Fig. 7, top left panel). With the suprathreshold C,

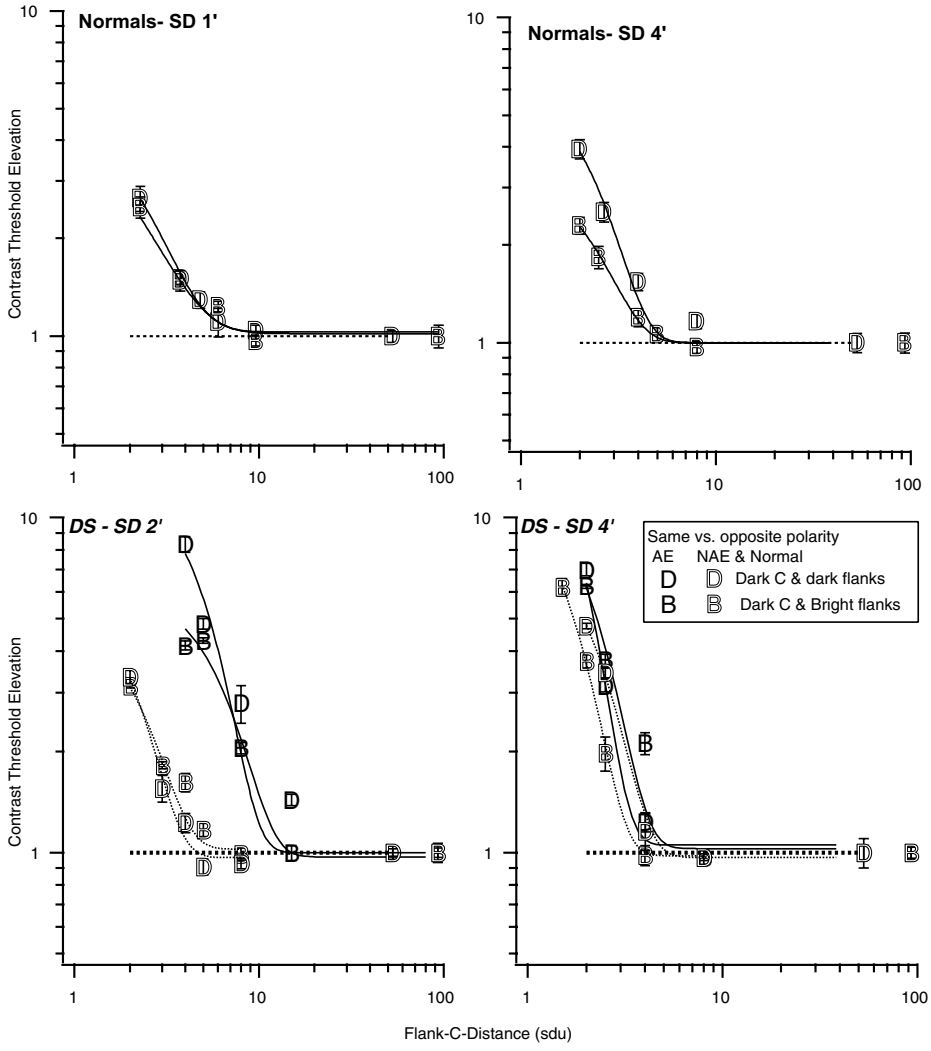

Fig. 7. The effect of flanker polarity. This figure shows the effect of flank polarity for near threshold and suprathreshold targets in normal observers (average data from three observers—top panel) and amblyope DS (bottom panel). Gray letters represent the data from amblyopic eye and black letters represent data from non-amblyopic eye.

contrast threshold elevation was smaller with opposite- than with same-polarity (Fig. 7, top right panel). With a near threshold C (Fig. 7, bottom left panel) opposite polarity flanks produce similar amounts of threshold elevation as same polarity flanks in the non-amblyopic eye of observer DS. The amblyopic eye of DS shows a greater extent of interaction and threshold elevation than his preferred eye with both polarities, and somewhat greater threshold elevation with same polarity than with opposite polarity flanks. With a suprathreshold C (Fig. 7, bottom right panel) there was very little difference in the magnitude of threshold elevation and extent of interaction between the two conditions or between the amblyopic and non-amblyopic eyes.

In order to determine whether the extent of crowding (critical distance) differs between same and opposite polarity flanks we fit the raw data with Gaussian functions (as described in Eq. (1)). The results are plotted as the critical distance estimates specified in minutes of arc between same vs. opposite polarity flanks (Fig. 8). From this figure we can see that the extent of interaction is slightly smaller with opposite polarity flanks for both the target sizes in our normal observers (open symbols coded for target size). For the larger C (0.44 deg in diameter), the extent of crowding with opposite polarity flanks reduced by 30–40% when compared to the extent of crowding with same polarity flanks for two normal observers, while one observer showed similar extents of crowding with same and opposite polarity flanks. For the smaller C (0.11 deg in diameter, small symbol) the extent of crowding with opposite polarity flanks was reduced by 10–20% for all the three control observers. The data of our amblyopes (gray open-NAE and solid-AE symbols coded for target size) shows that the extent of crowding scatters around the 1:1 line, showing that the extent of crowding is not very different between

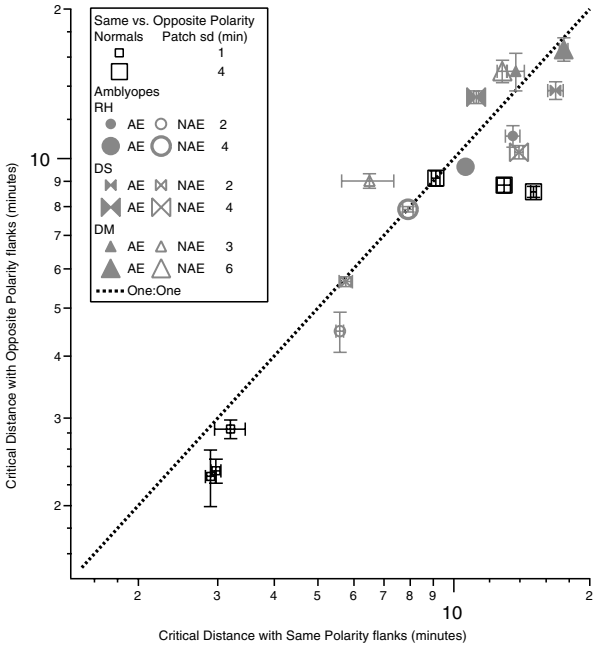

Fig. 8. The extent of crowding (i.e., the "critical distance" at which unflanked threshold doubled) specified in minutes of arc for the same (abscissa) vs. opposite (ordinate) polarity conditions. The diagonal line represents the one to one line. From this figure we can see that the extent of crowding is slightly reduced for both the target sizes (coded by symbol size) in our normal (open black symbols) and amblyopic observers (NAE-gray thick symbols, AE-gray solid symbols).

the same and the opposite polarity conditions for both target sizes. These results, in agreement with Hess et al. (2001) and Ehrt, Hess, Williams, and Sher (2003), show that for patterns that are larger than the acuity limit, crowding is not abolished by opposite polarity flanks. We note that for our targets the differences between the effect of same and opposite polarity flanks are small and variable and the extent of crowding measured with same and opposite polarity flanks do not differ systematically. Note too that our targets were not as small as those of Hess et al. (2000) and they did not have sharp edges.

Our amblyopic observers (Fig. 8) showed a greater extent of crowding in their amblyopic eyes for small targets, independent of flank polarity. Our results, in agreement with Hess et al. (2001), show that amblyopes show contour interaction irrespective of the polarity of the flanks. With our suprathreshold Gaussian C targets and flanks, the amblyopic observers showed similar extents of interaction when tested with same and opposite polarity flanks.

5. Experiment 2—Crowding with Gabor C-patterns

Experiment 1 showed that amblyopic observers exhibit a greater extent of crowding when compared to normal observers when tested with similar target sizes. This result with Gaussian targets is similar to previous studies, in that the stimuli are not band-limited, and therefore the increased extent of crowding may be a consequence of the visual system engaging large (low) spatial frequency filters (Flom et al., 1963; Hess et al., 2001). Hence, our primary goal in Experiment 2 was to test the extent of crowding using band-limited (Gabor) stimuli. Our band-limited (0.825 octaves) stimuli ensured that the initial (linear) filters selected in amblyopic vision were similar in scale to those selected for foveal viewing.

The target was a C-like figure comprised of 12 overlapped (equally spaced at 30 deg of angular separation) Gabor patches with one missing patch as in Experiment 1. On each trial the target was briefly presented (for 195 ms) in one of the two orientations: either a left vs. right or an up vs. down discrimination task. The two tasks were done in separate runs. The target carrier was always aligned with the C contour (see Fig. 2), and the radius of the C was always set at 3.33 times the patch standard deviation. The spatial frequency of the carrier varied between 2 and 10 c/deg.

In this experiment we measured the contrast threshold for identifying the position of the target gap using a two-alternative forced-choice method of constant stimuli. We used the 180-deg position discrimination task in order to eliminate the orientation cue, which is an important feature of the critical spatial frequency model (Bondarko & Danilova, 1997; Hess et al., 2000—discussed later).

The two surrounding flanks were comprised of one Gabor patch each. Unless otherwise specified the size, spatial frequency and orientation of the patches were identical to the missing patch in the target, and flank contrast was 90%. In left vs. right experiments, the flanks were placed on either side of the C and in the up vs. down experiments the flanks were placed above and below it. From run to run we varied the distance of the flanks from the target (specified as the distance from the center of the flank patch to the adjacent patch in the C that defines the gap). Fig. 2 (top panel) shows an example of targets and the flanks at 6, 4.5 and 3 standard deviation units. Both the target and the flanks were displayed at the same time for the same duration.

As in Experiment 1, the target was presented at one of the four near threshold contrast levels (based on pilot experiments), and the resulting psychometric function was fitted with a Weibull function in order to estimate threshold for identifying the orientation of the target. Each threshold estimate, corresponding to the contrast resulting in 81.6% correct performance, was based on 100 trials. All observers were tested for both the left/right and up/down position discrimination tasks in separate experiments. The contrast thresholds are weighted means of at least four individual threshold estimates. In

a control experiment we also measured the effect of changing the flank orientation with respect to the target's gap orientation.

6. Results and discussion—Experiment 2

The primary goal of this experiment is to ask whether the extended crowding in the amblyopic eye noted with Gaussian C's is a consequence of a shift in the spatial scale of analysis. Fig. 9 summarizes the results of this experiment by plotting the horizontal critical distance (abscissa—estimated as above for the left/right discrimination) vs. the vertical critical distance (ordinate)—estimated as above, for the up/down. Note that the critical distances are specified in standard deviation units. For the normals, the critical distances are slightly asymmetric (vertical smaller than horizontal) but are, on average about 2 SDU (strongly overlapped) as are the preferred eyes of the three amblyopes. The amblyopic eyes show an increased extent of crowding with these band-limited targets. The horizontal extent is, on average about twice that of the normals. The vertical extent shows individual differences. Two amblyopes have similar vertical and horizontal extent of crowding but RH shows a vertical extent in excess of 9 SDU! The large vertical extent of crowding suggests that it is not simply a consequence of smear due to unsteady (horizontal) fixation eye-movements.

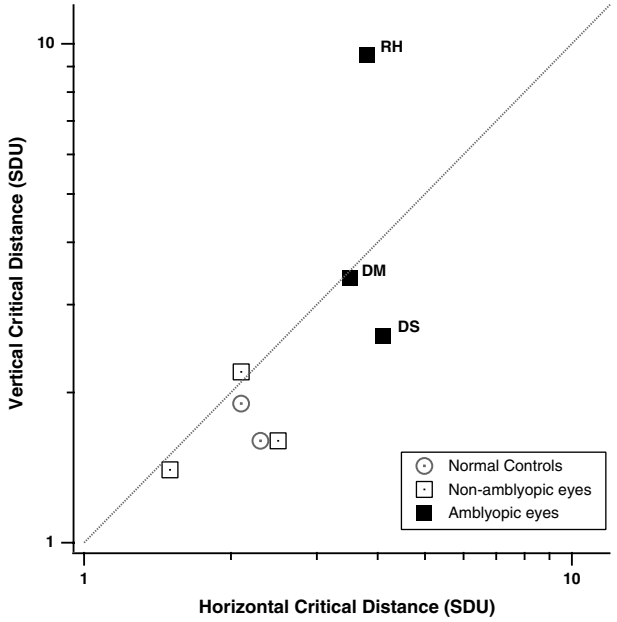

Fig. 9. Vertical extent of crowding (from the up vs. down task) vs. horizontal extent of crowding (from the left vs. right task) with Gabor C's for normal fovea (circles) non-amblyopic eyes (open squares) and amblyopic eyes (solid squares) are shown. Critical distances are specified in standard deviation units (SDU).

7. Experiment 3—Effect of flank orientation on crowding

In normal foveal vision, crowding with E-patterns is orientation specific. When the flank carrier orientation is orthogonal to the E-carrier orientation there is little or no threshold elevation (Levi, Klein, & Hariharan, 2002). In this experiment we also measured the effect of changing the flank orientation with respect to the C-target's gap orientation. For normal observer TL and the three amblyopic observers we tested crowding with C-patterns made of Gabor patches that were aligned to the curvature of the C (Fig. 2, top and middle panels). In the 'same' target and flank orientation condition (Fig. 2, top and lower panels) the flanks have the same orientation as the missing Gabor patch that makes the gap in the C-pattern. In the 'orthogonal' orientation condition, the orientation of the flank carrier was orthogonal to the missing Gabor patch that makes the gap. For example, the middle panel of Fig. 2 shows that in the first case (left) the missing Gabor patch (gap orientation) is horizontal, whereas the flanks are vertically orientated. Likewise, in the second case (right) the gap orientation is vertical, whereas the flanks are horizontally oriented. Other conditions were the same as Experiment 2.

Observer DL was tested with the C's and flanks made of horizontal carrier orientation as shown in the lower panel of Fig. 2. In the orthogonal target and flank orientation condition, the orientation of the flank carrier was vertical.

8. Results and discussion—Experiment 3

In normal foveal vision, crowding with C-patterns is orientation specific. For example, observer DL shows strong elevation when the gap orientation of the target and flanks are similar (dark bars in Fig. 10, top panel), but little or no elevation when flanks are orthogonal to the gap orientation of the C-pattern (striped bars in Fig. 10, top panel). Normal observer TL showed similar results. In contrast, orthogonally oriented flanks elevate thresholds in strabismic amblyopia (Fig. 10 lower panel). For example, with his amblyopic eye, observer DS had similar threshold elevation with both iso- (same) or orthogonally orientated flanks in the L/R task with his amblyopic eye, and shows substantial (more than a factor of two) threshold elevation with orthogonal flanks in the U/D task. The other amblyopic observers show similar threshold elevation with both iso- (same) and orthogonally oriented flanks.

9. General discussion

The main goal of our study was to compare the size dependence and specificity (polarity and orientation)

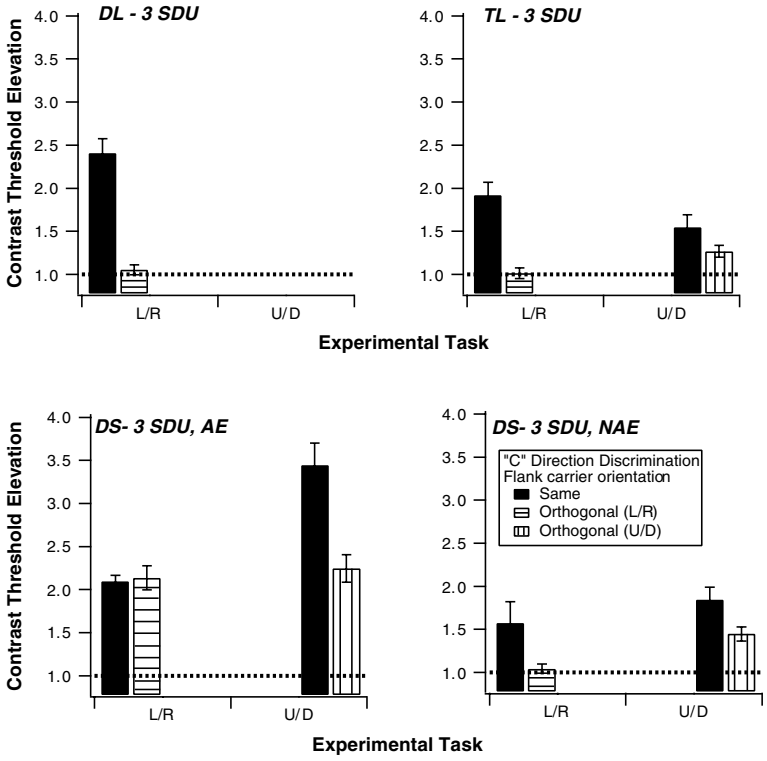

Fig. 10. The effect of flank orientation on contrast thresholds for identifying the location of the target gap in a Gabor C. Control observers (top panel) show less threshold elevation with orthogonally oriented flanks (striped bars) when compared to similar target and flank orientations (dark bars). Data from the up/down task for normal observer DL is not shown in the figure. This shows that crowding is orientation specific in normal observers. Amblyopic observer DS (lower panel). The left side of lower panel shows data from his amblyopic eye and the right side shows data from non-amblyopic eye. Like the control eyes the non-amblyopic eyes show orientation specificity for crowding. While the amblyopic eyes do not show a strong orientation preference.

of crowding in amblyopic observers to that of normal foveal and peripheral vision. In Experiment 1, we explored crowding, a form of inhibitory spatial interaction with low-pass Gaussian C-patterns in normal fovea, periphery and amblyopic observers. The main conclusions to be drawn from Experiment 1 are:

1. In normal fovea crowding extends over a small region and, once outside the "intrinsic blur" for crowding, the extent of crowding is proportional to target size, consistent with the results of Levi, Klein, and Hariharan (2002) using E-patterns.
2. In normal periphery and amblyopic visual systems crowding extends over inappropriately large spatial distances and does not depend on target size, consistent with recent studies (Levi, Hariharan, & Klein, 2002a, 2002b; Tripathy & Cavanagh, 2002).
3. In foveal and amblyopic vision the extent of crowding for our (suprathreshold) Gaussian C's is similar with same- and opposite- polarity flanks.

In order to test whether the greater extent of crowding seen in amblyopic visual system is a consequence of a scale shift to larger (lower) spatial frequency filters and to test the "critical spatial frequency" model, we measured and quantified extent of crowding using a band-limited C-pattern with no orientation cue in Experiment 2, leading to:

4. Crowding occurs over greater distances in amblyopes with band-limited C-patterns. Thus, the large extent of crowding seen in amblyopic observers from Experiment 1, is not simply a consequence of shift in the first stage (linear) spatial scale of analysis.

The present results confirm and extend previous studies by us and others, showing that crowding in amblyopic and peripheral vision extends over greater distances than in the fovea, even after scaling for resolution. Moreover, for our soft-edged targets, this crowding occurs with both same and opposite polarity flanks. Finally, we show that in amblyopic vision, crowding may be qualitatively different in the amblyopic fovea, in that it occurs for orthogonally oriented flanks.

9.1. Mechanisms of foveal crowding

Hess and colleagues (Hess, Dakin, & Kapoor et al., 2000; Hess, Dakin, & Tewfik et al., 2001) proposed a "critical spatial frequency model" for foveal crowding, which assumes that the visual system uses some representation of amplitude within a critical orientation/

spatial frequency band to determine the orientation of the target like the Landolt C. Below, we look at the utility of the Fourier approach in a more general sense.

9.2. Modeling foveal crowding

9.2.1. A Fourier model

In our previous paper, we found that the Fourier approach was not very helpful in explaining foveal crowding of E's (see Levi, Klein, & Hariharan, 2002). However, as we pointed out, the E-like target is unorthodox, and may not provide a good test for the Fourier approach. Thus, we applied the Fourier approach to our Gaussian C's (see Appendix A for details).

Figs. 11 and 12 show that the Fourier approach is no more helpful in understanding the crowding of a C than of an E. Fig. 11(A) shows the two-dimensional Fourier transforms of the pedestal (Eq. (A.4)) and of the test (Eq. (A.2)). The vertical line in the test pattern panel is at $f = 1.1$ c/deg where the test pattern is strongest. The color bar shows the Fourier transform of the test pattern with two patches is weaker than the pedestal with 12 patches. Fig. 11(B) shows the Fourier transform of the mask plus pedestal at four mask separations (2σ, 3σ, 5σ, and 10σ). The first three separations are those used in our experiments. The mask and pedestal have contrasts of 10% and 2% respectively (note that we use these values for illustrative purposes only). The right and left panels of Fig. 11(B) are for the case where the mask and pedestal have same and opposite polarity respectively. For a non-filter based version of the Fourier approach to be useful there must be regions in Fourier space where the information matches the human data. In order to detect the test pattern one must use regions of Fourier space near the vertical line. For well-separated masks (the last two panels of Fig. 11(B)) there must be regions where the pedestal plus mask must be small near the vertical line. For closely spaced masks (the first two panels of Fig. 11(B)) the pedestal plus mask must be large near the vertical line.

In order to facilitate viewing the critical regions near the vertical line, in Fig. 12 we replot the Fourier transforms along the vertical cut at $f = 1.1$ c/deg. The two upper panels are similar to those in Fig. 11(A) and (B) except now the x-axis is the mask vertical spatial frequency and the y-axis is the separation, similar to Fig. 11. The horizontal spatial frequency is fixed at $f = 1.1$ c/deg where the test pattern is maximal. The four horizontal black lines in Fig. 12 correspond to the four mask separations shown in Fig. 11(B). The Fourier amplitudes along these cuts in the upper two panels of Fig. 12 are the same as the corresponding values along the vertical cut in Fig. 11(B). The upper two panels are the absolute values of the values in the lower panels. The absolute values should be a good indicator of the masking magnitude in a simple Fourier based model of masking.

It is difficult to see any pattern in these plots that would explain the foveal crowding seen in our experiments. As seen in the left panel of Fig. 12, the maximal amount of masking would be expected for mask separations of 10σ in the case when mask and pedestal have the same polarity. That is clearly a nonsensical result.

The Fourier approach does have value in that it identifies the region of Fourier space where the test information is to be found. As pointed out by Anderson and Thibos (1999), and by Bondarko and Danilova (1997) different letters can have quite different spatial frequency regions that provide optimal detection of the relevant test signal. However, when strong irrelevant features are present such as provided by the pedestal or by a distant mask, the simple Fourier approach is not useful in predicting gross features of pattern discrimination.

9.2.2. An overlap masking model

Flom et al. (1963) proposed that foveal crowding occurs when there is an overlap between the target and the flanks in the same neural unit e.g. cortical receptive field and/or hypercolumn (Levi et al., 1985; Levi & Klein, 1985). This explanation predicts that crowding would occur over a large range of target sizes and that the extent of crowding would be proportional to the target size (as shown in Fig. 6). Thus, this explanation implies that crowding is essentially contrast masking by nearby flanks (rather than a superimposed mask), and will occur when there is overlap between the target and flank (either physically, or in the same neural unit) that obscures the cue. In a previous paper (Levi, Klein, & Hariharan, 2002) we showed when tested with an "E-pattern" that foveal crowding could be predicted by a test-pedestal model and validated the prediction by a two-patch masking experiment. This model showed that foveal crowding is essentially pattern masking.

Based on our results we propose that foveal crowding when tested with a "C-pattern" can be explained by using the same model (refer to Levi, Klein, & Hariharan, 2002 for a detailed description of the model). Our C-pattern has only one missing gap, which can be easily masked by the one-patch flankers corresponding to the gap positions. To illustrate this point, we have implemented a very simplistic model of foveal crowding, in which the strength of crowding is directly related to the degree to which the flank overlaps the center of the missing patch. The prediction for the masked threshold relative to the unmasked threshold is given by the formula:

$$\mathrm{Th}_{\mathrm{el}} = 1 + E * \exp(-\mathrm{sep}^2/2) \qquad (2)$$

where E is the threshold elevation for a fully overlapped target plus flank and sep is the separation between the mask center and the center of the missing patch in stand-

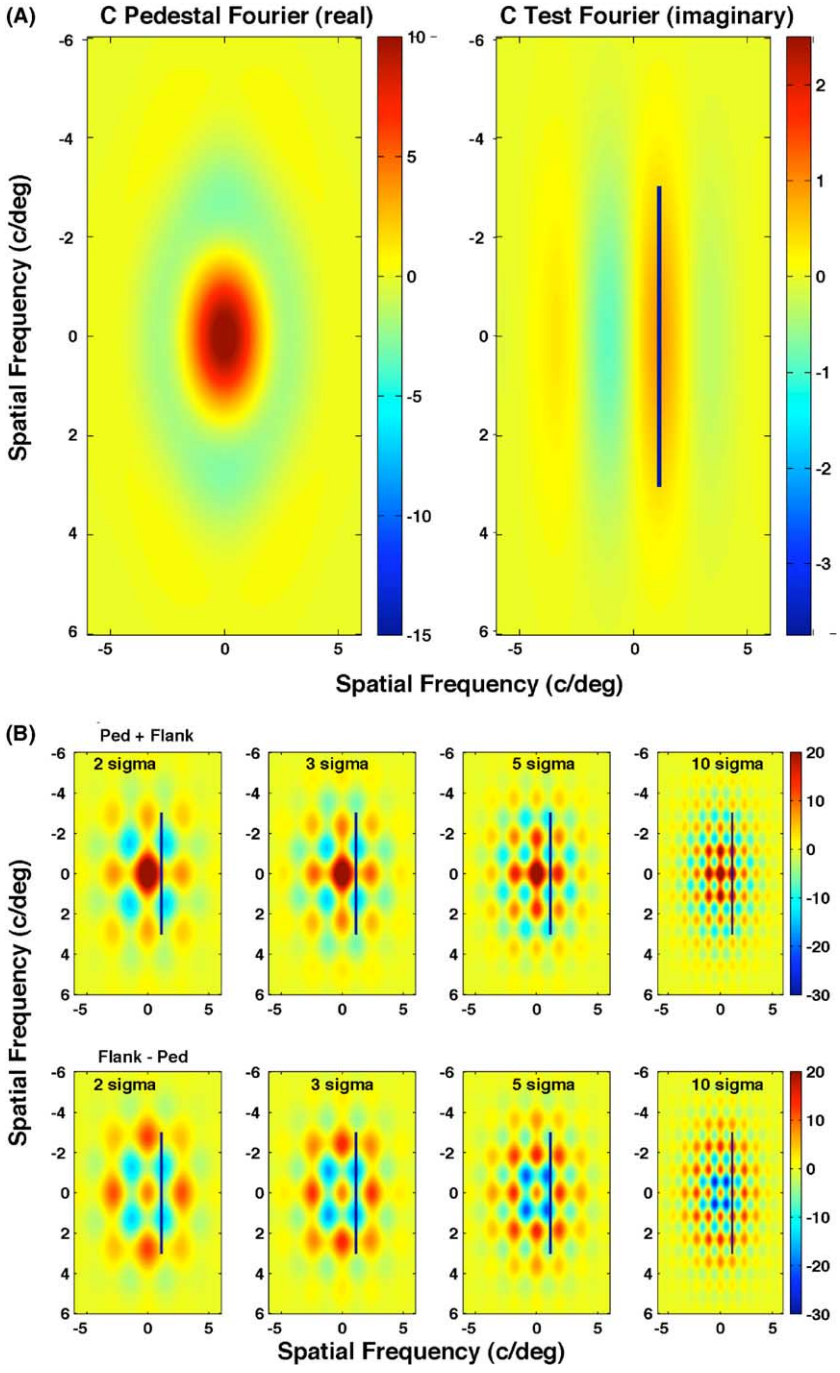

Fig. 11. (A) The two-dimensional Fourier transforms of the C-patterns. The left panel is the pedestal, the right panel is the test pattern. The vertical line in the test pattern panel is at $f = 1.1$ c/deg where the test pattern is strongest. (B) Fourier transform of the mask plus pedestal at four mask separations (2σ, 3σ, 5σ, and 10σ). The first three separations are those used in our experiments. The mask and pedestal have contrasts of 10% and 2% respectively. The upper and lower panels of Fig. 11(B) are for the case where the mask and pedestal have same and opposite polarity respectively.

ard deviation units. The three curves in Fig. 13 show ratios of 30, 20 and 10. The data are discrimination data of the 3 normal observers shown in Fig. 8 plus data of a fourth observer (MF) with same polarity targets only. Note that the model is almost certainly an oversimplification, and we are using it here only to illustrate the effects of overlap. Although the threshold elevation due to the physical overlap of target and mask can, in principle, explain foveal crowding at small separations (3 SDU and below), it does not explain the residual crowding that occurs up to about 5 SDU. This additional threshold elevation may be related to spatial uncertainty (the location of the cue is unknown) since our stimuli are briefly presented. The reader can see from Fig. 1, that

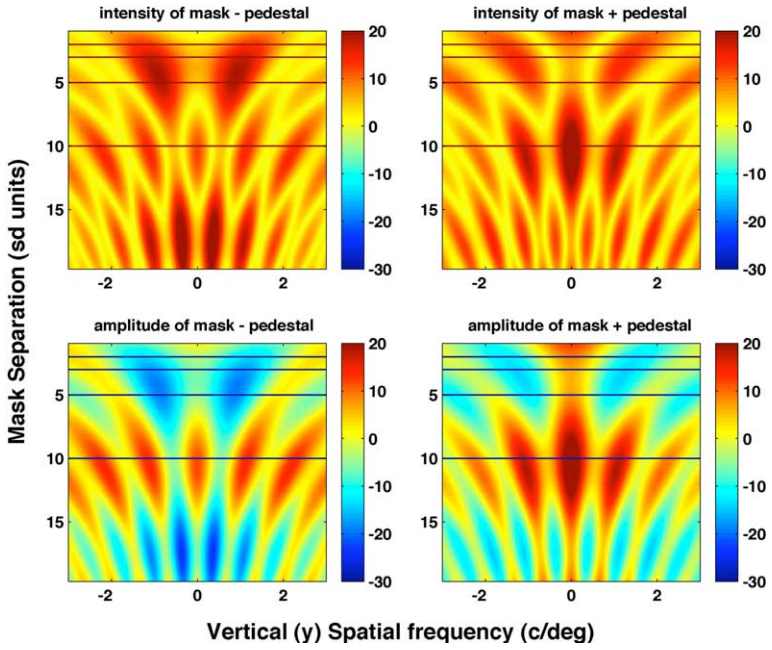

Fig. 12. The two-dimensional Fourier transform of the mask plus pedestal, along the vertical cut at $f = 1.1$ c/deg shown in Fig. 11. Lower panels: are similar to those in Fig. 11(B) except now the y-axis is the mask separation and the x-axis is the vertical spatial frequency. The four horizontal black lines correspond to the four mask separations shown in Fig. 11(B). The Fourier amplitudes along these cuts in the lower two panels of Fig. 12 are the same as the corresponding values along the vertical cuts in Fig. 11(B). Upper panels: Absolute values of the values in the lower two panels. The absolute values should be a good indicator of the masking magnitude in a simple Fourier based model of masking.

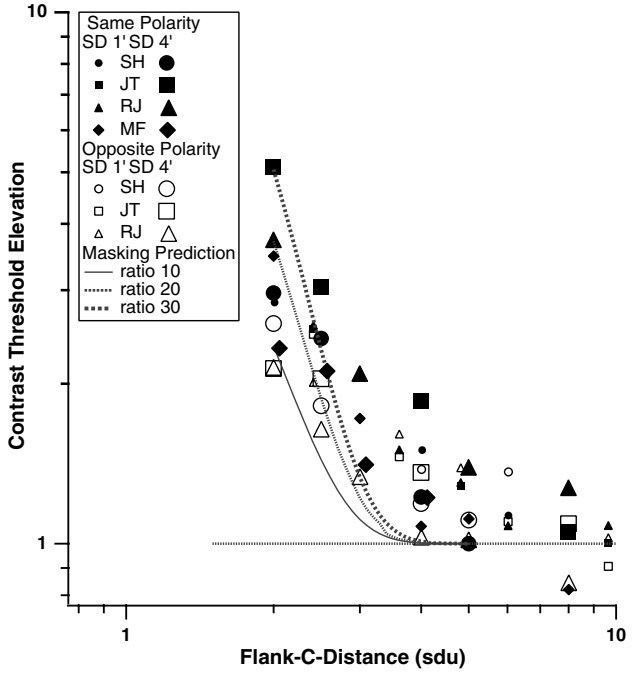

Fig. 13. An overlap model for crowding. The three curves show the predictions of a very simple model in which the strength of crowding is based on the overlap between target and flanks. The curves show ratios of 30, 20 and 10 (see text for details). The data are discrimination data of four normal observers for same (solid symbols) and opposite (open symbols) Gaussian C's.

with a long stimulus duration and scrutiny, there is little or no effect of flanks at 3 SDU. With brief durations and uncertainty about the locations of the target and mask, target and mask may get confused, and hence a "crowding effect". In the unflanked case there is no confusion. We note that this overlap model does not predict the bunching of foveal thresholds for different size targets (when plotted as a function of spatial separation) in the "crowding regime (Fig. 3) unless we postulate an "intrinsic blur" (Levi & Klein, 1990).

In contrast to the foveal crowding, the extent and strength of crowding seen in normal periphery (Experiment 1) and central field of amblyopic observers (Experiments 1 and 2) cannot be explained by simple pattern masking. In normal periphery and amblyopes crowding is not size dependent and it extends over greater distances, where there is no physical overlap between target and flanks. In peripheral vision, crowding may extend as far as 0.5 times the target eccentricity (Bouma, 1970; Toet & Levi, 1992; see Chung, Levi, & Legge, 2001 for a review), and the extent of interference increases much more rapidly than resolution as eccentricity increases (Latham & Whitaker, 1996). In the current study, the extent of interaction was approximately 8 percent of the eccentricity (dotted line in Fig. 5; see Levi, Hariharan & Klein, 2002a for a discussion of some of the factors that contribute to the large discrepancies in the reported extent of crowding). Based on these findings we propose a simple second stage pooling model in

which, the flanks and the target combine at a second stage of visual processing (Chung et al., 2001; Levi, Hariharan, & Klein, 2002a, 2002b; Parkes, Lund, Angelucci, Solomon, & Morgan, 2001; Pelli & Palomeres, 2000). An alternative formulation, is the hypothesis that crowding in peripheral (and amblyopic) vision represents an attentional limit (Tripathy & Cavanagh, 2002). These two ideas are not mutually exclusive (and may even be the same).

9.3. Second stage pooling and attentional resolution in peripheral and amblyopic vision

In normal fovea we seem to integrate features over just the region of an object needed to identify it. However, in the periphery and the amblyopic visual systems, where crowding is stronger, it seems that features are integrated over an inappropriately large area. He, Cavanagh, and Intriligator (1996) argued that perception of spatial details in the periphery is limited by two factors: (a) the ability of the visual system to resolve each feature (visual resolution), and (b) the ability of mechanisms at a subsequent stage, to isolate each feature, referred to as "attentional resolution" by Intriligator and Cavanagh (2001), who argued that peripheral crowding results from limitations set by attentional resolution. He et al. (1996) showed that perception of spatial details in the periphery is limited by visual resolution in the absence of distractors, while the perception of similar spatial details of a target depends on attentional resolution in the presence of distractors. Our results are consistent with the idea that crowding in peripheral and amblyopic vision reflects limited resolution at a stage beyond the initial filtering stage i.e. the feature extraction or detection stage (Chung et al., 2001; Parkes et al., 2001; Pelli & Palomeres, 2000; Tripathy & Cavanagh, 2002). In our crowding task our observers are required not only to detect the features, but also to localize the missing feature, which is the gap defining the orientation of the C-pattern in a 180-deg position discrimination task. In previous papers (Levi, Hariharan, & Klein, 2002a, 2002b) we showed that our amblyopic observers and normal observers in the periphery can easily detect the features under conditions where crowding is strong. Therefore, we suggest that the increased extent of crowding in amblyopic vision occurs because the target and the flanks are combined or pooled at a second stage of feature integration, which follows the feature extraction stage. In amblyopic vision, like the periphery, this pooling takes place over larger distances. The presence of crowding with band limited stimuli ensures that the large extent of crowding seen in amblyopic observers cannot be entirely explained by a shift in the spatial scale of analysis. We speculate that reduced contrast sensitivity in the amblyopic visual system at the feature extraction stage (detection), leads to a shift in spatial scale of analysis with broadband stimuli. The second (feature integration) stage is well matched to the target (Levi, Klein, & Carney, 2000), in normal fovea but not in peripheral or amblyopic visual systems because of limited resources. Our finding that crowding in normal fovea is qualitatively different from normal periphery and amblyopic visual system is consistent with Hess, Dakin, and Tewfik et al. (2001). Thus, the results from Experiment 2 using bandlimited stimuli shows that crowding is not just a consequence of a simple scale shift in the peripheral and amblyopic visual systems, instead it signifies a defective second stage filter that is not well matched to the target for identification.

Our conclusions receive some support from other psychophysical studies (Sharma, Levi, & Klein, 2000; Wong, Levi, & McGraw, 2001). For example, Sharma et al., 2000 tested the ability of amblyopic observers to count the number of missing patches from a uniform grid of 7×7 array of high contrast Gabor patches. The results showed that amblyopic observers underestimated the number of missing features to a greater extent when compared to the control observers from the uniform grid when $N > 4$ in the amblyopic eye. They suggested that tasks that involve identifying features in the presence of several other features (like counting the number of missing features) depend on the ability of attentional mechanisms to individuate or isolate each element, and they suggested that there may be a "higher" level deficit in strabismic amblyopia that reflected unreliable signals emanating from the representation of the amblyopic fovea in V1 as a consequence of abnormal visual experience. In the same vein, Wong et al. (2001) showed a detection loss in the amblyopic visual system for a second-order stimuli, that is thought to be processed at a stage beyond the initial filtering stage, probably V2 (Mareschal & Baker, 1999; Zhou & Baker, 1994). The amblyopic eyes showed a greater loss with the second-order stimuli when compared to the first-order stimuli, suggesting the presence of higher order deficits in the amblyopic visual system.

In summary, the large extent of crowding in peripheral and amblyopic vision may be a reflection of pooling information over a large (fixed) spatial area. This increased pooling could be a result of limited visual resources resulting in coarse "attentional resolution" (Intriligator & Cavanagh, 2001) in peripheral and amblyopic vision.

Acknowledgments

We are grateful to Hope Queener for programming these experiments. We also appreciate Tania La for participating and collecting data in these experiments. This research was supported by National Institutes Research Grants RO1EY01728 and RO1EY04776 and Core center grant P30EY07551. Commercial relationships: None.

Appendix A. Fourier transform of the "C-pattern"

The Appendix of Levi, Klein, and Hariharan (2002) provides full details on how we calculated the Fourier transform of E's. Here we apply this method to the 2AFC method of Experiments 2 and 3. We calculate the Fourier transform of C's comprised of 11 Gaussian patches (12 patches comprising a circle with either the rightmost or leftmost patch missing). The analysis for C's uses the same method used for E's, decomposing the C into a symmetric pedestal plus an anti-symmetric test. The pedestal is made symmetric by defining it as the average of a rightward and a leftward facing C. The test pattern is defined as the difference between the full C and the pedestal (i.e., the difference spectrum). For a rightward facing C the test pattern is an opposite polarity pair of Gaussian patches:

$$\mathrm{Test}(x,y) = c_{\mathrm{patch}}(g(x+r,y) - g(x-r,y))/2 \qquad (A.1)$$

where

$$g(x,y) = \exp(-(x^2+y^2)/2\sigma^2) \qquad (A.2)$$

The contrast of each patch is c_{patch} and $r = 3.3\sigma$ is the radius of the *C*. The factor of 1/2 in Eq. (A.1) is because the contrast of the two patches in the test pattern is half the contrast of the patches comprising the *C*. In this test-pedestal decomposition the 2AFC task becomes a task of discriminating the sign of the test pattern. The advantage of this decomposition is that the Fourier transforms of both test and pedestal are relatively simple.

The Fourier transform of test (x,y) in Eq. (A.1) is:

$$\mathrm{Test}(f,g) = \mathrm{i}c_{\mathrm{patch}}\sin(fr)G(f,g)/2 \qquad (A.3)$$

where

$$G(f,g) = \exp(-(f^2+g^2)\sigma^2/2) \qquad (A.4)$$

with f and g being the spatial frequencies in the horizontal and vertical directions respectively, in units of radians/deg, and σ being the spatial standard deviation in deg (same σ as Eq. (A.2)). Note that Eqs. (A.2) and (A.4) are Fourier transforms of each other, thus the standard deviations are reciprocals of each other. The $\mathrm{i} = \sqrt{-1}$ in Eq. (A.3) comes from the fact that the anti-symmetric test pattern produces a purely imaginary Fourier transform. The single term in Eq. (A.3) is able to represent a pair of Gaussians because the pair in Eq. (A.1) is anti-symmetric relative to the origin.

The Fourier transform of the pedestal comprised of 12 Gaussians is purely real and is given by:

$$\begin{aligned}\mathrm{Ped}(f,g) = c_{\mathrm{patch}}[&2\cos(\sqrt{3}fr/2)\cos(gr/2) + 2\\ &\times \cos(fr/2)\cos(\sqrt{3}gr/2)\\ &+ \cos(fr)/2 + \cos(gr)]G(f,g)\end{aligned} \qquad (A.5)$$

The term $\cos(fr)$ in Eq. (A.5) representing the rightmost and leftmost patches has half the contrast of the lowermost and uppermost patches because of the gap.

The Fourier transform of the mask is given by:

$$\mathrm{Mask}(f,g) = c_{\mathrm{mask}}\cos(f(m+r))G(f,g) \qquad (A.6)$$

where c_{mask} is the mask contrast and m is the distance from the mask center to the center of the patches in the closest C.

Note that in this model, the pedestal is present on all trials as is the mask. The pedestal has the same role as the mask. Nicely they are both symmetric functions so the Fourier transforms are real and thus the two add together simply. The test is anti-symmetric in space, and in Fourier space it is imaginary. So the task of distinguishing a leftward C from a rightward one (the "phase" task) is simply to determine the sign of the test in both space and frequency domain.

References

Anderson, R. S., & Thibos, L. N. (1999). Sampling limits and critical bandwidth for letter discrimination in peripheral vision. *Journal of Optical Society of America, A, 16*, 2334–2342.

Bondarko, V. M., & Danilova, M. V. (1997). What spatial frequency do we use to detect the orientation of a Landolt C? *Vision Research, 37*, 2153–2156.

Bouma, H. (1970). Interaction effects in parafoveal letter recognition. *Nature, 226*, 177–178.

Chung, S. T., Levi, D. M., & Legge, G. E. (2001). Spatial-frequency and Contrast properties of Crowding. *Vision Research, 41*, 1833–1850.

Ehrt, O., Hess, R. F., Williams, C. B., & Sher, K. (2003). Foveal contrast thresholds exhibit spatial- frequency- and polarity-specific contour interactions. *Journal of Optical Society of America, A, 20*, 11–17.

Flom, M. C., Weymouth, F. W., & Kahneman, D. (1963). Visual Resolution and Contour Interaction. *Journal of Optical Society of America, 53*, 1026–1032.

He, S., Cavanagh, P., & Intriligator, J. (1996). Attentional resolution and the locus of visual awareness. *Nature, 383*, 334–337.

Hess, R. F., & Jacobs, R. J. (1979). A preliminary report of acuity and contour interactions across the amblyope's visual field. *Vision Research, 19*, 1403–1408.

Hess, R. F., Dakin, S. C., & Kapoor, N. (2000). The foveal 'crowding' effect: physics or physiology. *Vision Research, 40*, 365–370.

Hess, R. F., Dakin, S. C., Kapoor, N., & Tewfik, M. (2000). Contour interaction in fovea and periphery. *Journal of Optical Society of America, A, 17*, 1516–1524.

Hess, R. F., Dakin, S. C., Tewfik, M., & Brown, B. (2001). Contour interaction in amblyopia: scale selection. *Vision Research, 41*, 2285–2296.

Hess, R. F., Williams, C. B., & Chaudhry, A. (2001). Contour interaction for easily resolvable stimulus. *Journal of Optical Society of America, A, 18*, 2414–2418.

Intriligator, J., & Cavanagh, P. (2001). The spatial resolution of visual attention. *Cognitive Psychology, 43*, 171–216.

Kooi, F. L., Toet, A., Tripathy, S. P., & Levi, D. M. (1994). The effect of similarity and duration on spatial interaction in peripheral vision. *Spatial Vision, 8*, 255–279.

Latham, K., & Whitaker, D. (1996). Relative roles of resolution and spatial interference in foveal and peripheral vision. *Ophthalmology Physiolological Optics, 16*, 49–57.

Leat, S. J., Li, W., & Epp, K. (1999). Crowding in central and eccentric vision: the effects of contour interaction and attention. *Investigative Ophthalmology and Visual Science, 40*, 504–512.

Levi, D. M., Klein, S. A., & Aitsebaomo, A. P. (1985). Vernier acuity, crowding and cortical magnification. *Vision Research, 25*, 963–977.

Levi, D. M., & Klein, S. A. (1985). Vernier acuity, crowding and amblyopia. *Vision Research, 25*, 979–991.

Levi, D. M., & Klein, S. A. (1990). Equivalent blur in amblyopic vision. *Vision Research, 30*, 1995–2022.

Levi, D. M., & Waugh, S. J. (1994). Spatial scale shifts in peripheral vernier acuity. *Vision Research, 34*, 2215–2238.

Levi, D. M., Waugh, S. J., & Beard, B. L. (1994). Spatial scale shifts in amblyopia. *Vision Research, 34*, 3315–3333.

Levi, D. M., Klein, S. A., & Carney, T. (2000). Unmasking the mechanisms for Vernier acuity: evidence for a template model for Vernier acuity. *Vision Research, 40*, 951–972.

Levi, D. M., Klein, S. A., & Hariharan, S. (2002). Suppressive and Facilitatory Spatial Interactions in Foveal Vision: Foveal Crowding is simple contrast masking. *Journal of Vision, 2*, 140–166.

Levi, D. M., Hariharan, S., & Klein, S. A. (2002a). Suppressive and facilitatory spatial interactions in peripheral vision: Peripheral crowding is neither size invariant nor simple contrast masking. *Journal of Vision, 2*, 167–177.

Levi, D. M., Hariharan, S., & Klein, S. A. (2002b). Suppressive and Facilitatory interactions in Amblyopic Vision. *Vision Research, 42*, 1379–1394.

Liu, L. (2001). Can amplitude difference spectrum peak frequency explain the foveal crowding effect. *Vision Research, 41*, 3693–3704.

Mareschal, I., & Baker, C. L. Jr. (1999). Cortical processing of second-order motion. *Visual Neuroscience, 16*, 527–540.

Parkes, L., Lund, J., Angelucci, A., Solomon, J. A., & Morgan, M. (2001). Compulsory averaging of crowded orientation signals in human vision. *Nature Neuroscience, 4*, 739–744.

Pelli, D. G., & Palomares, M. (2000). The role of feature detection in crowding. *Investigative Ophthalmology and Visual Science (Suppl.), 41*(4).

Sharma, V., Levi, D. M., & Klein, S. A. (2000). Undercounting features and missing features: evidence for a high-level deficit in strabismic amblyopia. *Nature Neuroscience, 3*, 496–501.

Toet, A., & Levi, D. M. (1992). The two-dimensional shape of spatial interaction zones in the parafovea. *Vision Research, 32*, 1349–1357.

Tripathy, S. P., & Cavanagh, P. (2002). The extent of crowding in peripheral vision does not scale with target size. *Vision Research, 42*, 2357–2369.

Wong, E. H., Levi, D. M., & McGraw, P. V. (2001). Is second-order spatial loss in amblyopia explained by the loss of first-order spatial input? *Vision Research, 41*, 2951–2960.

Zhou, Y. X., & Baker, C. L. Jr. (1994). Envelope-responsive neurons in areas 17 and 18 of cat. *Journal of Neurophysiology, 72*, 2134–2150.